Automated Control Matrix System Summary [DRAFT] T000105-??-D

Matt Evans

April 10, 2001

1 The Scope of This Note

This note is intended to explain the physics behind the lock-acquisition code which is currently running at LHO and elsewhere. It is not intended to be a general treatise on lock-acquisition nor is it intended to be a recipe for calibration or operation of the code.

2 Control Matrix Theory

The job of the "automated control matrix" is to invert the optical gain matrix, $\mathbf{G}$, and produce a control matrix, $\mathbf{M}$, which can be used to recover error signals for each degree of freedom, $\vec{D}$, from the outputs of the IFO, $\vec{O}$.

$$\vec{O} = \mathbf{G}\vec{D} \tag{1}$$

$$\vec{D} = \mathbf{M}\vec{O} \tag{2}$$

There are two steps to this process. The first is determining $\mathbf{G}$, which changes as a function of the fields in the IFO. The second is to invert $\mathbf{G}$. This step is non-trivial only because $\mathbf{G}$ may be singular. When $\mathbf{G}$ is singular only a subset of $\vec{D}$ can be produced from $\vec{O}$.

$$\vec{d} = \mathbf{m}\vec{o} \tag{3}$$

There are two fundamentally different types of singularities: "no signal" (NS) and "degenerate signal" (DS) singularities. NS singularities arise when there

is no comprehensible signal for some DOF (i.e. when a cavity is far from resonant, there is no good length signal). By definition, the process of lock acquisition begins with **m** of minimal dimension (usually 0 by 0), since none of the cavities in the system are locked, and ends after the removal of all NS singularities. DS singularities arise when two or more outputs of the IFO become linearly dependent (i.e. two signals contain the same information). This happens while the power in the IFO is building and renders one or more DOFs uncontrollable.

The general process of "lock acquisition" can be described as the expansion of **m** accomplished by the removal of NS singularities. In order for this process to occur there must be a path from the uncontrolled state to the fully controlled state along which **G** can be determined with sufficient accuracy to maintain control.

3 Lock Acquisition Path for LIGO 1

To place this discussion on firmer ground, this section will describe the lock acquisition path for the LIGO 1 IFO.

State 1	None of the degrees of freedom (DOFs) are controlled. This is the starting point for lock acquisition.
State 2	The recycling cavity DOFs (l_- and l_+) are controlled and the (first-order resonant) sidebands are resonant in the recycling cavity.
State 3	State 2 holds and one of the two arm cavity lengths is controlled. The carrier is resonant in the controlled arm cavity.
State 4	State 3 holds and the other arm cavity length is controlled. The carrier is resonant in both arm cavities and the recycling cavity. At the onset of this state all of the DOFs are controlled and all of the NS singularities have been removed from **G**. A DS singularity is, however, encountered in the course of the power buildup.
State 5	State 4 has endured long enough for the power level to equilibrate. This is the ending point for lock acquisition, though one would hope that the controllers used to achieve this state can hold it for some time.

The lock acquisition path for the LIGO 1 configuration was first described by Lisa Sievers in [LIGO 1 LSC FDR]. I have added "State 5" to Lisa's set of 4 states so that I can distinguish between the point at which all DOFs are controlled and the point at which stable lock has been achieved. The time between acquisition of State 4 and acquisition of State 5 for the Hanford 2k IFO is a few tenths of a second. The duration of this transition state corresponds to a frequency well within the bandwidth of the control loops and thus offers plenty of time for disaster to strike.

4 The Optical Gain Matrix

Elements of the optical gain matrix (OGM) are typically given by

$$G_{d_i \rightarrow o_j} = g_{output} \sum \gamma_{signal} \; A_{LO} \; A_{resonant} \tag{4}$$

where A_{LO} is the amplitude of the local oscillator at the output port, $A_{resonant}$ is the amplitude of the resonant field which generates signal sidebands, g_{signal} is the optical gain of the signal sidebands from the point of generation to the output port, and g_{output} is the fixed optical/electronic gain of the sensing hardware (i.e. pick-off reflectivities, photo-detector gain, filter gains, etc.).

The dominant elements of the OGM for the LIGO 1 IFO are[1]

$$G_{l_- \rightarrow Q_{ref}} = g_{lmRef} \; (A_{Cref} + A_{2ref}) \; A_{Srec} \; \gamma_{prm} \tag{5}$$

$$G_{l_- \rightarrow Q_{pob}} = g_{lmPob} \; A_{Crec} \; A_{Srec} \; \gamma_{prm} \tag{6}$$

$$G_{L_- \rightarrow Q_{asy}} = g_{Lasy} \; A_{Sasy} \; A_{C+} \tag{7}$$

$$G_{L_+ \rightarrow Q_{asy}} = g_{Lasy} \; A_{Sasy} \; A_{C-} \tag{8}$$

$$G_{l_+ \rightarrow I_{ref}} = g_{lpRef} \; (A_{Cref} - A_{2ref}) \; A_{Srec} \; \gamma_{prm} \tag{9}$$

$$G_{L_- \rightarrow I_{ref}} = g_{Lref} \; A_{Sref} \; A_{C-} \tag{10}$$

$$G_{L_+ \rightarrow I_{ref}} = g_{Lref} \; A_{Sref} \; A_{C+} \tag{11}$$

$$G_{l_+ \rightarrow I_{pob}} = g_{lpPob} \; A_{Crec} \; A_{Srec} \; \gamma_{prm} \tag{12}$$

$$G_{L_- \rightarrow I_{pob}} = g_{Lpob} \; A_{Srec} \; A_{C-} \tag{13}$$

[1]It will be assumed throughout this paper that $r_{ITMt} = r_{ITMr}$, $t_{ITMt} = t_{ITMr}$, and $r_{BS} = t_{BS} = \frac{1}{\sqrt{2}}$. I_{asy} seems to contain little unique information and, as a result, is not used and will not be considered further.

$$G_{L_+ \to I_{pob}} = g_{Lpob}\ A_{Srec}\ A_{C+} \tag{14}$$

where the C, S, and 2 subscripts indicate whether amplitude referred to is that of the carrier, first-order sidebands, or second-order sidebands[2]

$$A_+ = \gamma_t A_t + \gamma_r A_r, \tag{15}$$

[2]The amplitudes of the upper and lower sidebands are assumed to be equal at each port.

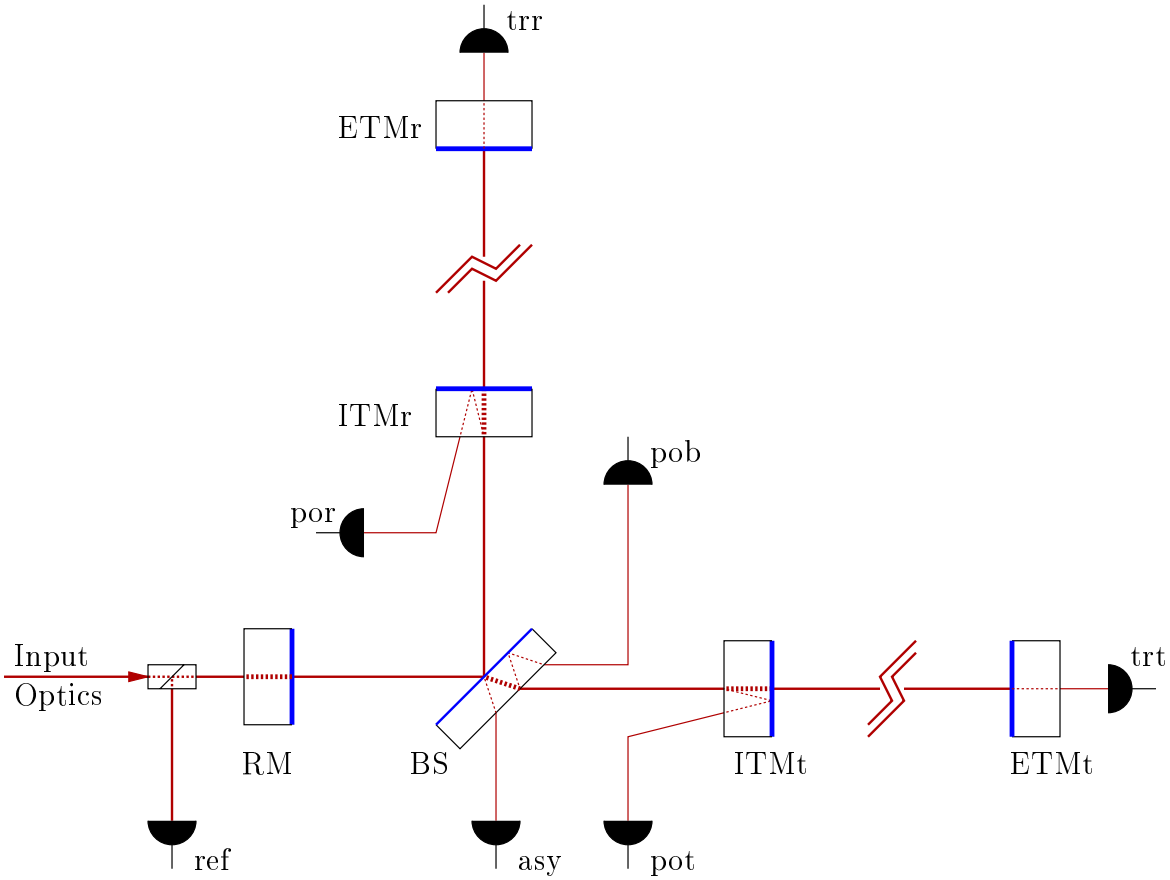

Figure 1: Sensor and mirror labels for the LIGO 1 IFO. For the 4km IFOs, the "t" (transmitted) arm is often referred to as the "x" or "right" arm, and the "r" (reflected) arm as "y" or "left" arm. For the 2km IFO the labels are reversed due to the presence of folding mirrors (not shown).

$$A_{-} = \gamma_t A_t - \gamma_r A_r, \tag{16}$$

$$\gamma_{\{t,r\}} = \left| \frac{1}{1 - r_{ITM} r_{ETM} e^{i\phi_{C\{t,r\}}}} \right| \tag{17}$$

$$\gamma_{prm} = \frac{r_{Smich}}{1 - r_{RM} r_{Smich}}, \tag{18}$$

r_{mich} is the reflectivity of the Michelson and arm cavities as a whole, A_{rec} is the amplitude of the recycling cavity field, A_{ref} is the amplitude of the reflected field, A_{asy} is the amplitude of the anti-symmetric field, $A_{\{t,r\}}$ are the amplitudes of the arm cavity fields, $\phi_{\{t,r\}}$ are the round trip phases in the arm cavity fields, and $g_{???}$ are constant gain coefficients.

5 Field Amplitude Estimators

The OGM is determined by seven field amplitudes (A_{Crec}, A_{Cref}, $A_{C\{t,r\}}$, A_{Srec}, A_{Sref}, A_{Sasy}), and three signal gains ($\gamma_{\{t,r\}}$, γ_{prm}). Each of these must be inferred from measurement, the more directly the better.

Measurements of the power transmitted through the ETMs will suffice as estimators of $A_{C\{t,r\}}$.

$$A_{C\{t,r\}} \simeq \sqrt{T_{ETM\{t,r\}}\ P_{tr\{t,r\}}}. \tag{19}$$

The primary assumption here is that contributions to the transmitted power from field components other than the carrier are negligible. This assumption is valid along the acquisition path, but is violated elsewhere.

To the degree that the recycling cavity is close to equilibrium

$$A_{Crec} \simeq \frac{\alpha_{Cin}\ t_{RM}}{1 - r_{RM} r_{Cmich}}\ A_{Cin}. \tag{20}$$

where A_{Cin} is the amplitude of the carrier field incident on the recycling mirror, and α_{Cin} is the mode-matching coefficient of the incident carrier into the recycling cavity. When neither arm cavity is resonant (state 2) the recycling cavity is anti-resonant for the carrier. In this state $r_{Cmich} \simeq -1$, which implies that

$$A_{Crec} \simeq \frac{t_{RM}}{1 + r_{RM}}\ A_{Cin}. \tag{21}$$

When only one arm cavity is resonant (state 3) $r_{Cmich} \simeq 0$ and

$$A_{Crec} \simeq \alpha_{Cin}\ t_{RM}\ A_{Cin}. \tag{22}$$

When both arm cavities are resonant (states 4 and 5) r_{Cmich} is close to, but less than one by a small and variable amount. A robust estimator for A_{Crec} in these states can be derived from the arm cavity amplitudes. Since

$$A_{C\{t,r\}} = \frac{\alpha_{C\{t,r\}}}{\sqrt{2}} \; \frac{t_{ITM}}{1 - r_{ITM} r_{ETM}} \; A_{Crec}, \tag{23}$$

where $\alpha_{C\{t,r\}}$ are mode-matching coefficients for the arm cavities,

$$A_{Crec} \simeq \sqrt{2} \; \frac{1 - r_{ITM} r_{ETM}}{t_{ITM}} \; max \left[A_{C\{t,r\}} \right], \tag{24}$$

assuming that at least one of $\alpha_{\{t,r\}} \sim 1$.

The signal gain in the arm cavities, for signal frequencies less than the cavity pole frequency, is essentially the same as the carrier gain. That is

$$\gamma_{C\{t,r\}} \simeq \frac{\sqrt{2} \; A_{C\{t,r\}}}{A_{Crec}} \tag{25}$$

Demodulation of the beam-splitter pick-off field at twice the modulation frequency produces a signal which is proportional to the first-order sideband power in the recycling cavity, S_{pob}.

$$A_{Srec} \simeq \sqrt{g_{Spob} \; S_{pob}} \tag{26}$$

This signal is a valid estimator only when $|A_{Crec} \; A_{2rec}| \ll A_{Srec}^2$. This condition is satisfied at all points on the acquisition path after the acquisition of state 2.

Since the Michelson asymmetry provides a fairly constant loss, A_{Sasy} can be estimated directly from A_{Srec}.

$$A_{Sasy} \simeq A_{Srec} \; sin \left[2\pi \frac{\Delta_{mich}}{\lambda_{mod}} \right], \tag{27}$$

where $\Delta_{mich} \simeq 0.3m$ is the Michelson asymmetry and $\lambda_{mod} \simeq 10m$ is the modulation wavelength.

Similarly, r_{Smich} can be approximated as

$$r_{Smich} \simeq cos \left[2\pi \frac{\Delta_{mich}}{\lambda_{mod}} \right] \tag{28}$$

in the estimation of γ_{Sprm}.

The two reflected field amplitudes (A_{Cref}, A_{Sref}) are each estimated in two parts, the mode-matched part and the non-mode-matched part. The amplitude of the mode-matched reflected fields are

$$A_{refMM} = r_{RM}\alpha_{in}A_{in} - t_{RM}r_{mich}A_{rec} \tag{29}$$

and the amplitude of the non-mode-matched reflected fields are

$$A_{refNM} = \sqrt{1-\alpha_{in}^2}A_{in}. \tag{30}$$

For the sidebands, the mode-matching coefficient can vary substantially. This coefficient is computed from A_{Srec} and A_{Sin} using

$$\alpha_{in} = \frac{(1 - r_{RM}r_{mich})A_{rec}}{t_{RM}A_{in}}. \tag{31}$$

With α_{Sin} in hand, A_{SrefMM} and A_{SrefNM} can be computed directly from equations (29) and (30).

The reflected carrier amplitudes cannot be computed in the same way since r_{Cmich} is unknown. α_{Cin} is, however, a much more stable quantity and much closer to unity than α_{Sin} and as a result it can simply be assigned a value (e.g., $\alpha_{Cin} = 1$). Further complexity is added by the existence of the reflected power measurement, P_{ref}, which should satisfy

$$P_{ref} = A_{CrefMM}^2 + A_{CrefNM}^2 + A_{SrefMM}^2 + A_{SrefNM}^2. \tag{32}$$

Since P_{ref} is typically dominated by A_{CrefMM}, it seems plausible that equation (32) can be used to produce a more robust measure of A_{CrefMM} (up to a sign ambiguity) than indirect computation via equation (29). This strategy is, in fact, the one used at LHO. (The sign ambiguity is resolved by taking the sign of A_{CrefMM} given by solving (31) for r_{mich} and using the result in (29).)

We are still in need of an equation which relates A_{refMM} and A_{refNM} to A_{ref}. Unfortunately, the mode-matched and non-mode-matched components of the reflected fields will both contribute to the signal and they will do so in a way that depends on the geometry of the fields when they arrive on the photo-detector. The degree to which the non-mode-matched fields contribute is relegated to an input fudge-factor via

$$A_{ref} = A_{refMM} + \alpha_{sigNM}\ A_{refNM}. \tag{33}$$

Measurement of α_{sigNM} remains a technical challenge.

CURRENT LHO SETUP

The amplitudes currently in use (shown with a bar) are related to the ones described above by:

$$\bar{A}_{Crec} = \frac{A_{Crec}}{t_{RM} J_0 \gamma} \tag{34}$$

$$\bar{A}_{Casy} = \frac{A_{Casy}}{t_{RM} J_0 \gamma} \tag{35}$$

$$\bar{A}_{Cref} = \frac{A_{Cref}}{J_0 \gamma} \tag{36}$$

$$\bar{A}_{C\{t,r\}} = \sqrt{2}\, \frac{1 - r_{ITM} r_{ETM}}{t_{ITM} t_{RM}}\; max\left[A_{C\{t,r\}}\right] \tag{37}$$

$$\bar{A}_{Crec} = \frac{A_{Crec}}{t_{RM} J_1 \gamma} \tag{38}$$

$$\bar{A}_{Casy} = \frac{A_{Casy}}{t_{RM} J_1 \gamma} \tag{39}$$

$$\bar{A}_{Cref} = \frac{A_{Cref}}{J_1 \gamma} \tag{40}$$

This should be of no consequence to operators of the system.

6 Calibration of Power Signals

Three power measurements ($P_{tr\{t,r\}}$ and P_{ref}) and one demodulated signal (S_{pob}) are used in the field amplitude estimators described above. Since S_{pob} is difficult to calibrate directly, a power measurement at the same port, P_{pob}, will be also be needed. Each of these must be calibrated to some fiducial input power. The calibrated measurements are not in any particular units; they are relative to the fiducial input. Furthermore, these calibrations are chosen so as to eliminate many optical parameters from the gain calculations.

The reflected power and the pick-off power are calibrated with both ITMs misaligned and the RM aligned. In this configuration

$$P_{ref} = r_{RM}^2 \tag{41}$$

and

$$P_{pob} = t_{RM}^2 . \tag{42}$$

> CURRENT LHO SETUP: P_{pob} is actually P_{poy}, so it should be calibrated with the all mirrors except ITMy misaligned. In this configuration $P_{pob} = P_{poy} = 1$.

The transmitted arm power calibration $\bar{P}_{tr\{t,r\}} = \alpha^2_{\{t,r\}}$ is performed by misaligning one ITM and the RM, then locking the aligned arm. If the mean alignment is good $\bar{P}_{tr\{t,r\}} \simeq 1$ when the power is at its highest points (i.e. $\alpha^2_{\{t,r\}} \sim 1$). QPD readout noise should be removed or ignored. This calibration removes the properties of the ITMs and ETMs from all gain calculations and changes equation (24) to

$$A_{Crec} \simeq t_{RM} \ max \left[\sqrt{\bar{P}_{tr\{t,r\}}} \right] . \tag{43}$$

To calibrate S_{pob}, the ETMs should be misaligned and the recycling cavity locked (first-order sidebands resonant). In this state

$$S_{pob} \simeq \frac{P_{pob}}{2} \tag{44}$$

where the factor of 2 compensates for the presence of two first-order sidebands.

> CURRENT LHO SETUP: $S_{pob} \simeq \frac{P_{pob}}{2J_1(\gamma)}$
> Use test output 10 for S_{pob} calibration (i.e. make the test output ~ 1 in state 2).

7 Implementation

This section discusses the implementation details of the automated control matrix algorithm. The algorithm performs two types of actions: continuous changes in the control matrix which compensate for continuous changes in the OGM, and discontinuous changes which result from the addition or removal of a singularity in the OGM. The discontinuous changes occur at the state boundaries discussed in section §3 and near the DS singularity that appears during state 4. Each of these discontinuous changes is marked in the algorithm by a state bit and recognized via a trigger of some sort.

7.1 Discontinuous Changes: Triggers and Bits

The state progression begins with the departure from state 1. As the recycling cavity becomes resonant, S_{pob} increases and it remains at an elevated level all along the acquisition path. Note that this is a demodulated signal and, as a result, the carrier field beating with the second-order sidebands produces a negative output. This fact makes S_{pob} a particularly good indicator of state 2 since spurious carrier resonances in the recycling cavity are easily rejected. For these reasons, the trigger which recognizes the transition from state 1 to state 2 and beyond is based on the value of S_{pob}. This trigger has distinct on and off levels to prevent noise from toggling the state. These levels are called "recOn" and "recOff" and the associated bit is "Engaged." To be painfully clear, the Engaged bit is set anytime $S_{pob} > T_{recOn}$ and is reset anytime $S_{pob} < T_{recOff}$.

State 3 is entered when one of the two arms becomes resonant for the carrier. The power buildup in the cavity, as measured by the transmitted power signal, $\bar{P}_{tr\{t,r\}}$, is used to recognized the approach of resonance ($\bar{P}_{tr\{t,r\}} > T_{armOn}$) and the passage of resonance ($\bar{P}_{tr\{t,r\}} < T_{armOff}$). The corresponding state bits are labeled "ArmTOn" and "ArmROn." When one of these bits is set, along with the Engaged bit, the IFO is in state 3.

Entry into state 4 is indicated when both arm bits and the Engaged bit are set. The passage of the DS singularity in state 4 is marked by the "InvBad" bit. This bit is set anytime the absolute value of the normalized determinant of the OGM is less than the threshold value "detNormMin." Also in the course of state 4 the l_- degree of freedom must transition from Q_{ref} to Q_{pob} to avoid a zero in the reflected signal. This transition is accomplished by simply switching signals at a predetermined arm power level dubbed "lmPO."

7.2 Continuous Changes: The Control Matrix in Each State

7.2.1 State 1: Not Engaged

In this state the OGM is essentially unknown so there is little to be done but wait for state 2 to happen by chance. At LHO some excitation is necessary and is provided by setting

$$M_{I_{ref} \to l_+} = c_{push}/g_{lpRef} \tag{45}$$

and

$$M_{Q_{ref}\to l_-} = c_{push}/g_{lmRef} \tag{46}$$

where c_{push} is an adjustable parameter.

7.2.2 State 2: Engaged

In state 2 l_- and l_+ are controlled. l_-, being rather separate in the OGM is dealt with separately. Until state 4 the error signal for l_- is produced entirely from Q_{ref} via

$$M_{Q_{ref}\to l_-} = 1/G_{l_-\to Q_{ref}}. \tag{47}$$

This leaves a 1x1 control matrix for l_+. In this state its error signal comes from I_{ref} via

$$M_{I_{ref}\to l_+} = 1/G_{l_+\to I_{ref}}. \tag{48}$$

7.2.3 State 3: Engaged and one Arm Locked

Here the 1x1 control matrix containing l_+ expands as one NS singularity is removed from the OGM. The resulting 2x2 matrix produces error signals for l_+ and L_+ ($L_- = \pm L_+$ depending on which arm is producing the signal).

$$\begin{bmatrix} l_+ \\ L_+ \end{bmatrix} = \begin{bmatrix} G_{l_+\to I_{ref}} & G_{L_+\to I_{ref}} \\ 0 & G_{L_+\to Q_{asy}} \end{bmatrix}^{-1} \begin{bmatrix} I_{ref} \\ Q_{asy} \end{bmatrix}. \tag{49}$$

7.2.4 States 4 and 5: Engaged and both Arms Locked

As state 4 is entered and the last NS singularity is removed from the OGM the control matrix expands again to become 3x3.

$$\begin{bmatrix} l_+ \\ L_+ \\ L_- \end{bmatrix} = \begin{bmatrix} G_{l_+\to I_{ref}} & G_{L_+\to I_{ref}} & G_{L_-\to I_{ref}} \\ G_{l_+\to I_{pob}} & G_{L_+\to I_{pob}} & G_{L_-\to I_{pob}} \\ 0 & G_{L_+\to Q_{asy}} & G_{L_-\to Q_{asy}} \end{bmatrix}^{-1} \begin{bmatrix} I_{ref} \\ I_{pob} \\ Q_{asy} \end{bmatrix}. \tag{50}$$

As the determinant of the 3x3 OGM shown above becomes small the signals for l_+ and L_+ become inseparable. This DS singularity forces a choice between controlling L_+ or l_+. Since L_+ dominates in both I_{ref} and I_{pob}, and since it is by far the more sensitive degree of freedom, the error signal equation is reduced to

$$\begin{bmatrix} L_+ \\ L_- \end{bmatrix} = \begin{bmatrix} G_{L_+\to I_{ref}} & G_{L_-\to I_{ref}} \\ G_{L_+\to Q_{asy}} & G_{L_-\to Q_{asy}} \end{bmatrix}^{-1} \begin{bmatrix} I_{ref} \\ Q_{asy} \end{bmatrix}, \tag{51}$$

and l_+ is left uncontrolled until the DS singularity passes. As the determinant once again becomes significantly different from zero the control matrix returns to its 3x3 form.

When $\bar{P}_{tr\{t,r\}}$ increases beyond T_{lmPO}, l_- is switched to Q_{pob} by setting $M_{Q_{ref} \to l_-} = 0$ and

$$M_{Q_{pob} \to l_-} = 1/G_{l_- \to Q_{pob}}. \tag{52}$$

8 Gain Coefficient Measurement

All of the sensing gain constants, $g_{???}$, can be measured in either state 2 or state 3. The L_+ and L_- control loops should have similar filters and identical DC gains. As state 4 progresses the pole in the L_+ optical transfer function will move from the one-arm-cavity pole to the coupled-cavity pole. Either the loop shape should be changed or the loop should be made stable with either pole.